Space Dependent Effects on the Lawson Criterion, the Ignition Condition, and Thermal Equilibria in Tokamaks

R.W. Conn and Jay Kesner

December 1975

UWFDM-155

To be published in *Nuclear Fusion.*

FUSION TECHNOLOGY INSTITUTE

UNIVERSITY OF WISCONSIN

MADISON WISCONSIN

Space Dependent Effects on the Lawson Criterion, the Ignition Condition, and Thermal Equilibria in Tokamaks

R.W. Conn and Jay Kesner

Fusion Technology Institute
University of Wisconsin
1500 Engineering Drive
Madison, WI 53706

http://fti.neep.wisc.edu

December 1975

UWFDM-155

To be published in *Nuclear Fusion.*

Space Dependent Effects on the Lawson Criterion, the Ignition Condition, and Thermal Equilibria in Tokamaks

Jay Kesner

Robert W. Conn

December 1975

Fusion Technology Program
Nuclear Engineering Department
University of Wisconsin
Madison, Wisconsin 53706

Abstract

The sensitivity of the Lawson and ignition criteria to plasma density and temperature profiles is examined and it is found that peaked profiles lead to a considerable easing of these criteria, as well as to a significant increase in the average fusion power density. A space and time dependent tokamak transport program is then used to investigate the expected profiles in a tokamak reactor when the dominant transport mechanism is trapped particle driven turbulence. It is found that thermally stable profiles exist within a fairly narrow range of mean density and with mean temperatures of 8 to 15 keV. The profiles are found, in fact, to be sharply peaked at the center due to alpha heating and to rapid diffusion near the edge. This is advantageous from the viewpoint of meeting either the Lawson criterion or the ignition condition in tokamaks. The equilibria are found to be very sensitive to the size of the device and to the conditions imposed at the plasma edge. They are also somewhat sensitive to the fueling profile that is imposed. A detailed comparison is also made between tokamak plasma equilibrium parameters predicted by often used global energy balance models and by space dependent calculations. It is found that the global model results can differ sharply from the space dependent calculations with regard to mean temperature, mean density, particle confinement time and fractional burnup. In particular, the fractional burnup from global calculations can be a factor of 10 too high and this can have an important detrimental impact on the anticipated tritium inventory and refueling systems in tokamaks.

I. Introduction

In order to analyze a power producing fusion reactor, it is important to consider the spatial profiles of temperature and density in the plasma. Lawson's criteria[1] for "break-even" in a driven reactor and the criterion for plasma ignition both depend upon these spatial profiles. As we will see, for a given plasma energy content, it becomes easier to "break-even" or ignite the plasma as the temperature and density profiles become more peaked. Furthermore, with a beta limited plasma such as a tokamak, the average fusion power density is found to increase for more peaked profiles and the maximum value of the power density occurs at lower average plasma temperatures.

There are many factors that will determine the profile of density and temperature in a thermally stable plasma fusion device. First are the scaling laws; the size of the device and the coefficients for conduction and convection for both particles and energy. Second the conditions at the plasma edge will play an important role in the equilibrium which the plasma will assume. In a tokamak, for example, this might mean the presence of a limiter, a gas blanket,[2] or a divertor.[3,4] Thirdly, if there is an energy or density source necessary to maintain equilibrium, the source profile will effect the plasma equilibrium.

In Section IIa, we will discuss the numerical model used to obtain the equilibrium profiles and in Section IIb, a global energy balance model used for comparative calculations is described. The effect that spatial profiles have on Lawson and ignition criteria will be discussed in Section III. In Section IV, we will discuss the results of detailed calculations of the thermal equilibria assumed by a reactor size tokamak plasma. We have assumed in these calculations that diffusion and conduction losses for particles and energy are dominated by the presence of turbulence due to trapped particle microinstabilities. We will discuss how the equilibrium is effected by

machine size, boundary conditions and the shape of a particle source profile. As we will show, the temperature and density profiles may be much more peaked than observed in present-day tokamaks and this fact will play a favorable role in evaluating the feasibility of tokamak reactors. We compare results from space dependent and global models for tokamak plasmas in Section V and summarize in the last section.

II. Numerical Model of Tokamak Plasmas

a. Space Dependent Model

The tokamak discharge is represented by a set of transport equations for electrons and ions in cylindrical geometry with spatial dependence admitted in the radial direction. These equations are time dependent and thermally stable solutions are found by examining the approach to equilibrium. Although it is not certain that the equilibrium profiles attained in this way are unique, the same equilibrium was found in all cases where different initial conditions or different time steps were used.

The equations to be solved include ion and electron power balance equations, the diffusion equation for the ion density, Faraday's Law, Ampere's Law, Ohm's Law, and a charge neutrality equation. They may be written as follows:

$$\frac{\partial n_e T_e}{\partial t} = 4.28 \times 10^{-11} n_e n_i \frac{(T_i - T_e)}{T_e^{3/2}} + \frac{1}{1.5r} \frac{\partial}{\partial r} \left(r n_e \chi_e \frac{\partial T_e}{\partial r}\right) - \frac{1}{r} \frac{\partial}{\partial r} (r n_e V_e T_e)$$

$$+ 4.17 \times 10^{15} \{n_D n_T \langle \sigma v \rangle U_{\alpha e} + \underline{E} \cdot \underline{J} + P_{inj} \left(U_{be} + f\left(\frac{E_\alpha}{E_b}\right) U_{\alpha e}\right) \qquad (1)$$

$$- P_I - P_B - P_S - P_L - P_R\}$$

$$\frac{\partial n_i T_i}{\partial t} = -4.28 \times 10^{-11} n_i n_e \frac{(T_i - T_e)}{T_e^{3/2}} + \frac{1}{1.5r} \frac{\partial}{\partial r} (r n_i \chi_i \frac{\partial T_i}{\partial r}) - \frac{1}{r} \frac{\partial}{\partial r} (r n_i V_i T_i)$$

$$+ 4.17 \times 10^{15} \{n_D n_T \langle \sigma v \rangle_{DT} U_{\alpha i} + P_{cx} + P_{inj} (U_{bi} + f(\frac{E_\alpha}{E_B}) U_{\alpha i})\} \quad (2)$$

$$\frac{\partial n_i}{\partial t} = -\frac{1}{r} \frac{\partial}{\partial r} (r n_i V_i) \quad (3)$$

$$n_i V_i = -D \frac{\partial n_i}{\partial r} \quad (4)$$

$$\frac{\partial B_\theta}{\partial t} = 10^5 \times \frac{\partial E}{\partial r} \quad (5)$$

$$\frac{\partial J}{\partial t} = 7.96 \times 10^4 \frac{1}{r} \frac{\partial}{\partial r} (r \frac{\partial E}{\partial r}) \quad (6)$$

$$E = \eta_{NC} J \quad (7)$$

$$n_e = n_i + 2n_\alpha + \sum_i n_{Z_i} Z_i \, . \quad (8)$$

$T_{e,(i)}$ is the electron (ion) temperature (eV), B_θ is the poloidal magnetic field (gauss), $n_{e,(i)}$ is the electron (ion) density (cm^{-3}), V_i is the ion velocity (cm/ms), J is the toroidal current density (amp/cm^2), E is the toroidal electric field (volt/cm), r is the radius (cm), t is time (ms), $\chi_{e,(i)}$ is the electron (ion) thermal diffusivity (cm^2/ms), η_{NC} is the neoclassical resistivity (ohm-cm), D is the diffusion coefficient (cm^2/ms), $U_{bi,(e)}$ is the fraction of beam energy going to ions (electrons), $U_{\alpha i,(e)}$ is the fraction of alpha energy going to ions (electrons), and f is the fraction of deuterons(tritons) in the neutral beam which undergo fusion as they slow down in the target plasma.

P_B, P_S, P_L, and P_R represent bremsstrahlung, synchrotron, line and recombination radiation, respectively (watts), P_{cx} is the energy loss due to charge exchange (watts), and S is the source of cold plasma ($cm^{-3}ms^{-1}$) due to a cold plasma source or neutral particle reflux.

The neoclassical resistivity η_{NL} is given by[5]

$$\eta_{NL} = 0.0103 \quad \frac{\ell n\Lambda}{T_e^{3/2} f_T} \left(\frac{.457\ Z_{eff}}{1.077 + Z_{eff}}\right) + .29\ Z_{eff}) \text{ ohm-cm} \tag{9}$$

with

$$f_T = 1 - \{1.95 \sqrt{\frac{r}{R}} + .95\ (r/R)\}/(1 + \nu^*) \tag{9a}$$

$$\nu^* = 6.92 \times 10^{-14}\ Z_{eff}\ \frac{R^{3/2} B_T n_e \ell n\Lambda}{\sqrt{r}\ B\ T_e^{\ 2}} \tag{9b}$$

and

$$Z_{eff} = \frac{\sum n_j Z_j^2}{n_e} \ . \tag{9c}$$

R is the toroidal major radius (cm) and $\ell n\Lambda$ is the coulomb logarithm, f_T is the correction to the resistivity due to particle trapping, and ν^* is the ratio of collision frequency to bounce frequency. The differential equations for the plasma behavior are solved using a Crank-Nicholson method in which the differential equations are linearized and transformed into an implicit set of difference equations.[6]

The transport coefficients (D, χ_e, χ_i) are treated implicitly and are assumed to vary in functional form as the plasma changes in collisionality. The high collisionality regime that is used reflects pseudoclassical scaling[7] and, as the plasma heats, the transport is assumed to be caused by turbulence, passing successively into regimes dominated by the presence of the trapped electron mode,[8] trapped ion mode[9] and the collisionless trapped particle interchange mode.[10] Transport coefficients based on estimates of the linear growth rates for these modes has been summarized by Dean et al.[11] In the

trapped electron regime, the relationship between χ_i and χ_e is not known. Rather than optimistically assuming χ_i remains neoclassical in this regime, we have taken $\chi_i = \varepsilon \chi_e$ where ε is the local aspect ratio.

Throughout the calculations, we have fixed the current profile as parabolic and ignored magnetic field diffusion. This was permissable because the ohmic heating term which is dependent on the local current density is insignificant at the high temperatures attained in ignited tokamaks, and therefore the thermal equilibrium is not effected by the ohmic heating profile. Furthermore, the trapped ion mode turbulent transport is the dominant energy loss mechanism in the outer part of the plasma and this mode is independent of the poloidal magnetic field.

Although the code is capable of studying magnetic field diffusion, the time scale for current penetration is very long and furthermore, for high beta plasmas, equations 5 through 7 do not properly describe this process since they do not include a poloidal dependance. A proper calculation of the current profile would involve solution of the MHD equilibrium problem, as described in references 12 and 13 . By ignoring current diffusion, we are able to significantly reduce the required computer time.

Heating of the plasma by 3.5 MeV alpha particles produced from D-T fusion reactions have been included with the assumption that the energy is deposited in the plasma instantaneously and at the place of birth of the particles. The profile of alphas within the plasma is obtained by a solution of a diffusion equation which uses the same transport coefficients as for the ions.

The thermal equilibration term and the D-T fusion terms in the energy balance equations are evaluated assuming that these processes are classical. It is conceivable that in a turbulent plasma they may be enhanced. However, this would not be expected to significantly effect the equilibrium. A more detailed description of the computer code is given in reference 14.

b. Space Independent, Global Energy Balance Model

A much simpler tokamak program can sometimes be utilized in which the space dependence is eliminated from equations (1) and (2) and the resulting equations are solved using Newton's method. The radial dependence is eliminated in the following manner:

1. For the conduction terms:

$$\frac{2}{3}\frac{\partial}{\partial r} rn\chi \frac{\partial T}{\partial r} \rightarrow \frac{\bar{n}\hat{T}}{\tau_c} \tag{10a}$$

with $\tau_c = a^2/4\chi(\bar{n},\hat{T})$

2. For the convection terms:

$$-\frac{1}{r}\frac{\partial}{\partial r}(rnvT) \rightarrow \frac{\bar{n}\hat{T}}{\tau_D} \tag{10b}$$

with $\tau_D = a^2/4D(\bar{n},\hat{T})$

3. The equilibration, radiation, fusion and ohmic heating terms are evaluated assuming parabolic profiles for the density and temperature:

$$n(r) = 2\bar{n}\,(1 - r^2/a^2)^2 \tag{10c}$$

$$T(r) = 2\hat{T}\,(1 - r^2/a^2)^2 \tag{10d}$$

Equations of this type have been described in our earlier work.[15,16]

III. Lawson and Ignition Criteria

The basic condition required of a plasma to approximately achieve break-even is typically given by the Lawson criteria.[1] A plasma at a local temperature $T(r)$ composed of electrons at density $n(r)$ and deuterons and tritions at density $n(r)/2$, respectively, has an average thermal energy of approximately $\overline{3n(r)kT(r)}$ if all species have the same temperature. Here, k is the Boltzmann constant and the bar indicates a volumetric average. Such a plasma will radiate via many processes but for the purpose here, let us assume that bremsstrahlung radiation is the main loss mechanism. Let us assume further that the thermal energy, $\overline{3nkT}$, is contained for a characteristic time of τ_E. Then one must balance $P_B + \frac{\overline{3n_e kT}}{\tau_E}$ against the energy generated in the plasma to maintain energy equilibrium.

Fusion reactions take place at the rate $\overline{n(r)^2 \langle \sigma v(T(r)) \rangle}$ and an amount of energy E_{fus} is released per fusion reaction. Assuming that this power plus bremsstrahlung and plasma thermal energy is available for conversion to electricity at an overall efficiency, η, the Lawson criteria arises from the following energy balance:

$$\frac{\overline{3nkT}}{\tau_E} + P_B = \eta \{ \frac{\overline{n^2 \langle \sigma v \rangle}}{4} E_{fus} + \bar{P}_B + \frac{\overline{3nkT}}{\tau_E} \} \qquad (11)$$

For the case of a cylindrical plasma of radius a, the barred quantities are defined by

$$\bar{f} = \frac{1}{\pi a^2} \int_0^a f(r) 2\pi r dr. \tag{11a}$$

This then gives

$$\bar{n}_e \tau_E = \frac{3\bar{n}_e k \overline{n(r)T(r)}}{\eta \frac{n^2 \langle \sigma v \rangle}{4} E_{fus} - \bar{P}_B (1-\eta)} . \tag{11b}$$

If we choose, for example, $n(r) = \bar{n} f(r)$ and $T(r) = \hat{T} f(r)$ with $f(r) = (1 + \delta)(1 - r^2/a^2)^{\delta}$, we find

$$\bar{n}\tau_E = \frac{3kT\overline{f^2}(1-\eta)}{\eta f^2 \langle \sigma v \rangle E_{fus}/4 - C\hat{T}^{1/2}\overline{f^{5/2}}(1-\eta)} \tag{12}$$

where we have used $P_B = C \overline{n^2 T^{1/2}}$. Noting that the mean temperature ($\bar{T}$) is given by

$$\bar{T} = \frac{\int_0^a n(r)T(r)rdr}{\int_0^a n(r)rdr} = \frac{(\delta+1)^2 \hat{T}}{(2\delta+1)} \tag{13}$$

we see that $\bar{n}\tau_E$ is a function only of the mean temperature and the functional form of the radial dependence of temperature and density. A plot of $\bar{n}\tau_E$ versus $\bar{T}$ is shown in Fig. 1. The parameter δ characterizes the sharpness of the radial profiles and $\delta = 0$ corresponds to uniform conditions as assumed in formulating the Lawson criteria. Notice that whereas the minimum of $\bar{n}\tau_E$ in the usual Lawson curve (when $\delta = 0$) occurs at about 5×10^{13} cm^{-3}-s with $\bar{T}$ of about 25 keV, for more peaked profiles ($\delta > 1$) $\bar{n}\tau_E$ is reduced by a factor of 2 to 5 and the $\bar{n}\tau_E$ value of 5×10^{13} will occur below 10 keV mean temperature.

The ignition condition requires the alpha energy generated within the plasma to balance the total plasma energy losses. This condition may be written as

$$\frac{\overline{3nkT}}{\tau_E} + P_x = \overline{n^2\langle\sigma v\rangle}\, E_\alpha/4 \qquad (14)$$

E_α is the energy of the alpha particle produced by each fusion event (3.5 MeV). The $\bar{n}\tau_E$ for ignition satisfies the criterion

$$\bar{n}\tau_E = \frac{\overline{3nkT}}{\overline{n^2\langle\sigma v\rangle}\, E_\alpha/4 + \overline{Cn^2T^{1/2}}} = \frac{3\,\hat{T}\,\overline{f^2}}{\overline{f^2\langle\sigma v\rangle}\, E_\alpha/4 + C\hat{T}^{1/2}\overline{f^{5/2}}} \qquad (15)$$

This again is a function of mean temperature and the peaking factor δ, and is shown in Fig. 2. Notice that, as with the Lawson criteria, $\bar{n}\tau_E$ is reduced by a factor of 2 to 5, the minimum $\bar{n}\tau_E$ for ignition moves down from 1.5×10^{14} in the flat profile ($\delta = 0$) case to below 6×10^{13}, and an $\bar{n}\tau_E$ value below 1.5×10^{14} can be found in the 6 to 10 keV temperature range for $\delta > 2$.

In a tokamak experiment, the poloidal beta (β_θ) may be limited by MHD stability conditions to less than the plasma aspect ratio. The parameter β_θ may be written as

$$\beta_\theta = 4 \times 10^{-10}\, \frac{a^2\overline{nT}}{I^2} = 4 \times 10^{-10}\, \frac{a^2\bar{n}\,\hat{T}\,\overline{f^2}}{I^2} \quad . \qquad (16)$$

with I, the toroidal plasma current, expressed in Amperes.
The power density generated by fusion reactions can then be expressed in terms of β_θ as

$$P = \frac{\overline{n^2\langle\sigma v\rangle}}{4} E_{fus} = 1.56 \times 10^{18}\, \frac{I^4\,\beta_\theta^2}{a^4\hat{T}^2}\, \frac{\overline{f^2\langle\sigma v\rangle}}{(\overline{f^2})^2} \qquad (17)$$

The power density is a function only of the mean temperature and the peaking factor, and is shown on Fig. 3. Notice that the power density may be a factor of 2 to 5 higher in the more peaked cases compared with the $\delta = 0$ case. Furthermore, the maxima occur at somewhat lower temperatures for the more peaked profiles. These calculations all serve to indicate that when profiles are more peaked, the constraints on ignition and power density are considerably relaxed.

IV. Thermal Equilibria in Tokamaks

As we have seen in the previous section, peaked density and temperature profiles have a marked effect on the behavior of large fusion plasmas. We have used the space-time transport code described in Section II to determine the equilibrium profiles one may expect in large tokamaks. We have also considered the physical processes which may be expected to play an important role in determining these profiles.

In the calculations presented here it is assumed that the plasma scaling is dominated by the presence of trapped particle driven turbulence. The thermal equilibria are therefore basically a balance of the alpha power generated in the plasma and the conduction and convection losses. These losses are largely determined by the value of the diffusion coefficient and the thermal diffusivity at the plasma edge. The assumption of the presence of trapped particle dominated turbulence is considered to be a worst case assumption in that the turbulent transport coefficients are much larger than the equivalent neoclassical or pseudoclassical coefficients. The use of these coefficients do, however, lead to thermal equilibrium near the peak of the power density curves, whereas when transport is classical (or pseudoclassical)

a tokamak will ignite and heat to very high temperatures until synchrotron radiation balances alpha power.[17] The beta limit on such systems then requires a very low plasma density and therefore a low fusion power density. In all of the calculations to be presented, we have used an aspect ratio of 3, a toroidal magnetic field of 40 kG (on axis), and a safety factor q at the plasma edge of 2.5.

In the first set of calculations, we have tried to model a divertor by the following boundary conditions. We define characteristic lengths for ion temperatures, electron temperature and density respectively at the plasma edge as

$$L_i = \left.\frac{T_i}{\nabla T_i}\right|_{r = a} \tag{18a}$$

$$L_e = \left.\frac{T_e}{\nabla T_e}\right|_{r = a} \tag{18b}$$

$$L_n = \left.\frac{n}{\nabla n}\right|_{r = a} \tag{18c}$$

At the plasma-divertor boundary, the density equation is approximately given by $D(a)\,\frac{\partial^2 n}{\partial r^2} = \frac{n}{\tau_D}$ where τ_D is the time an ion spends in the divertor zone before being collected. Setting $\frac{\partial^2 n}{\partial r^2} \approx n/L_D^2$ gives $L_D \approx \sqrt{\tau_D D(a)}$. Estimates indicate this length will be between 5 and 50 cm, depending on the diffusion coefficient and the time spend by the ion in the divertor zone, that is, whether a fraction of the ions which step into the divertor region mirror during a collision time, or whether loss cone instabilities develop and quickly deflect them into the loss cone.[18] In our calculations, we have conservatively chosen L_n to be 50 cm. The electron temperature is expected to have a similar characteristic length as the

density, since sheaths are expected to develop at the divertor collector plates which will serve to repel all but the most energetic electrons and therefore drop the electron temperature in the divertor zone.[18] We have therefore also taken L_e = 50 cm. For the ions, there does not appear to be any mechanism associated with the divertor which degrades their energy so we have taken L_i = 1000 cm. It will be seen, however, that rethermalization serves to keep the ion temperature close to the electron temperature.

These boundary conditions turn out to be equivalent to assuming low values for the temperature and density at the plasma edge and lead to peaked profiles. If smaller values of L_e and L_n has been used, the edge density and temperature would have been lower and the resulting profiles would have been even more peaked.

Figure 4 shows the equilibrium density and temperature profiles for a plasma with a minor radius of 5 m. Notice that they are quite peaked which in turn will cause the fusion power density to be even more sharply peaked (Figure 5), with 90% of the total power being generated within 15% of the plasma volume. Table 1a summarizes the main parameters for three 5 m minor radius tokamak cases (numbered a, b, and c) and for two 4 m tokamaks (d and e). The peak temperature is typically a factor of 5 or 6 above the edge value, and the peak density is typically a factor of 50 above the edge value. The concave behavior exhibited by these profiles is in large part a result of the diffusion coefficients, which increase rapidly in moving toward the plasma edge, as seen in Fig. 6. The minimum which occurs at about r/a = 0.1 represents the region beyond which trapped particle modes become the dominant transport mechanism. Below a mean density of $5 \times 10^{13} cm^{-3}$ in the 5 m case and $7 \times 10^{13} cm^{-3}$ in the 4 m case, ignition cannot be attained.

Figure 7 indicates the total poloidal beta (due to electrons, ions and alphas) found for the equilibrium solutions as a function of the mean temperature.

It is known that as the poloidal beta approaches the aspect ratio (assumed to be 3) it will become difficult to find MHD stable solutions. Therefore, if the very stringent scaling laws that we have chosen are applicable, there will probably not exist a stable MHD equilibrium for a 4 m minor radius reactor, whereas a 5 m plasma does possess stable solutions with mean temperatures of 6 to 7 keV and densities of 4 to 5 x $10^{13} cm^{-3}$.

The very high plasma loss rates caused by adverse scaling laws and a sharp density fall off at the divertor boundary will lead to very short particle and energy containment times in these systems. As Table 1b indicates, the particle containment time is typically less than a second. However, the time required for a particle to move from the centerline to the plasma edge is 10 to 15 seconds. Since the slowing down time of 3.5 MeV alphas is the order of 1 second and since most of the alphas are generated in the central region of the plasma, it is still reasonable to assume that the alpha particles deposit their energy near the flux surface on which they were produced.

We have considered the effect that maintaining the plasma edge density at a higher level would have on reactor operation. This might be the case for example with the gas blanket concept.[2] As is seen in Fig. 8, as the edge density rises from 5 x $10^{12} cm^{-3}$ to 4 x $10^{13} cm^{-3}$, the plasma loss rate (and therefore the fueling rate) decreases by a factor of 10. Details of these calculations are shown in Table 2. If the plasma edge density is kept high enought to invert the density profile, trapped particle modes and drift wave like modes may disappear resulting in much reduced energy transport and the system will then heat up to the synchrotron radiation equilibrium level.

In these calculations, we have assumed that the rapid loss of ions is balanced by some fueling mechanism, such as injecting pellets,[19] which serves as a source of cold plasma. We have looked at the effect that varying the source profile will have on the equilibrium that the plasma will attain. It is seen that the power produced and the plasma beta are not strongly dependent on the injection profile. Figure 8 shows three source profiles ranging from a parabolic to a flat profile. As the fueling profile becomes more peaked, it is seen that the plasma density will also peak up and will thereby cause enhanced particle and energy loss. The enhanced particle loss rate requires an increased fueling rate, and the energy necessary to heat the fuel up to the local temperature causes both the peak and the mean temperature to drop. This lowers β_θ and the power output. When the plasma source is peaked towards the edge as seen in Figure 9, a similar effect is noted. The density profile in the central region of the plasma flattens (but does not invert). This causes a lower energy outflux which in turn causes the central region to heat and the mean beta and power density to increase.

V. Comparison of Space Dependent and Space Independent Calculational Models

Global balance tokamak models, similar to the one described in Section II-B, have been used in many tokamak design studies.[15,16,20] We are therefore interested in examining the validity of these simplified models. In fact, we find that the global balance code gives results that are in many important ways quite different from the space dependent calculations, a not too surprising result. It was noted in Section II-B, the global balance model assumed parabolic temperature profiles. This is not consistent with the results of the space dependent calculations just described. Furthermore, the transport coefficients in the simple model are evaluated at the mean temperatures and mean density

whereas these transport coefficients should properly be evaluated at the plasma edge to determine particle and heat flow out of the plasma.

For example, it was found using the space dependent calculations that the minimum mean density for ignition of a 4m minor radius tokamak was 7×10^{13} and for a 5m minor radius machine, it was 4×10^{13} cm^{-3}. In contrast, the minimum density for ignition given by the global balance code for the 4 and 5m tokamaks were $3 \times 10^{13} cm^{-3}$ and $2 \times 10^{13} cm^{-3}$, respectively. This discrepancy is largely due to the fact that the transport coefficients for the global balance model are evaluated at the mean density instead of the edge density. Near the edge, the collisionality is such that the transport is dominated by trapped particle driven turbulence for which $D_\perp \sim \chi \sim T^{7/2} \nabla n^2 / n^3$.

Table 3 contains a comparison of plasma parameters derived from a global energy model and a space dependent program for a tokamak with a minor radius of 5m, an aspect ratio = 3, a toroidal field of 40 kG, a safety factor at the plasma edge of 2.5, and mean density of $4 \times 10^{14} cm^{-3}$. In each case, thermally stable equilibria are found but in the global model, the mean temperature, the beta value and the plasma energy content are a factor of 2 to 2.5 times higher. Furthermore, although the energy containment time in the global model is 20% below the value predicted by the space dependent model, the particle containment time is nearly a factor of 5 larger. These factors cause the fractional burnup predicted by the spacial model to be a factor of 10 smaller than in the global calculations, which means that the amount of tritium tied up in the refueling cycle of a tokamak may be much larger than heretofore suspected. Clearly, this can have an important effect on the design of tritium handling systems for near term as well as full scale power systems.

In sum, the results here shows that space dependent tokamak transport calculations may give very different, and perhaps more pessimistic, results than

a simplified global energy balance mode. In particular, the particle containment time and fractional burnup can be much shorter than expected and the conditions required for ingition can be more stringent.

VI. Conclusions

The spacial profiles that plasmas assume are quite important in evaluating the performance of these systems as reactors. The relatively peaked density and temperatures that are seen in many present day experiments would significantly lower the Lawson and ignition criteria and increase the mean fusion power density for ingited plasmas.

The equilibria assumed in large tokamaks have been examined for several cases. These equilibria are seen to depend sensitively on the scaling laws chosen the physical size of the device and the conditions at the the plasma edge, and to be somewhat dependent on the fueling profile. When the dominant transport process in a tokamak is trapped particle driven turbulence, thermally stable equilibria are seen to exist within a fairly narrow range of β_θ at mean temperatures close to the peak of the beta limited power density curves. With these scaling laws, a divertor is found to impose on the plasma a very peaked density profile. This will cause a rapid loss of particles and energy from the system which in turn would greatly enhance the problem of fueling and of collecting the high flux of energy which would appear at the divertor collector plates. Furthermore, the small particle containment time (less than 1 second) results in a very low fractional burnup in the system and this will greatly enhance the tritium recycle rate, the tritium inventory and therefore the tritium handling problems of reactor systems.

If the divertor could be eliminated and the plasma edge density maintained at a sufficiently high level, the plasma energy and particle loss rates could be reduced but this would lead to other difficulties such as providing sufficient pumping of the vacuum chamber, preventing the plasma from contacting the wall, and preventing impurity influx which would surely come about from bombardment by charge exchanged neutrals. If an energy source were necessary to drive the

reactor, the equilibria would be expected to be sensitive to the shape of the energy source.

Finally, the sapce dependent plasma calculations have been compared with predictions of a much simpler energy balance model and it is found that the space dependent analysis gives much more pessimistic results with respect to particle containment time, fractional burnup, and ignition conditions.

Acknowledgement

Research supported by the Electric Power Research Institute under EPRI contract 741220.

References

1. J. D. Lawson, Proc. Phys. Soc. 70 (1957) 6.

2. B. Lehnert, Nuc. Fus. 8, (1968) 173.

3. C. R. Burnett et al., Phys. Fluids 1, (1958), 438.

4. B. Badger et al., "UWMAK-I, A Wisconsin Toroidal Fusion Reactor Design," UWFDM-68, Nuclear Engineering Dept., Univ. of Wisconsin (1973).

5. R. Hazeltine, F. Hinton, M. Rosenbluth, Phys. Fluids, 16 (1973) 1645.

6. M. M. Widner, R. A. Dory, Bull. Am. Phys. Soc. 11 (1970) 1418. See also, Oak Ridge Nat'l. Lab Report ORNL-TM-3498 (1971).

7. L. Artsimovich, J.E.T.P. Letts. 13 (1971) 70.

8. B. B. Kadomtsev, O. P. Pogutse, Nuc. Fus. 11 (1971) 67.

9. B. B. Kadomtsev, O. P. Pogutse, Sov. Phys. Dokl. 14 (1969) 470.

10. J. D. Callen, B. Coppi, R. Dagazian, R. Gajewski, D. J. Sigmar, in Plasma Physics and Controlled Nuclear Fusion, (Proc. Madison Conf., June 1971)(IAEA, Vienna, 1972)Vol. II, 451.

11. S. O. Dean et al. "Status and Objectives of Tokamak Systems for Fusion Research," U. S. Atomic Energy Commission, WASH-1295 (1974).

12. J. D. Callen and R. A. Dory, Phy. Fluids 15, (1972) 1523.

13. M. S. Chance et al., "Study of Magnetohydrodynamic Modes in Tokamak Configurations with Noncircular Cross Sections," in Plasma Physics and Controlled Nuclear Fusion 1974 (Proc. 5th Int. Conf. Tokyo, 1974) 1, IAEA Vienna (1974) 463.

14. R. W. Conn, M. Khelladi, J. Kesner, UWFDM-136, Univ. of Wisconsin, Madison (1975). Submitted to Nucl. Fusion.

15. B. Badger et al., "UWMAK-I, A Wisconsin Toroidal Fusion Reactor Design," Nucl. Eng. Dept. Report UWFDM-68 (Univ. of Wisconsin, Nov. 1973) Chapter II. See also, B. Badger et al., "UWMAK-II, A Conceptual D-T Fueled Helium Cooled Tokamak Power Reactor Design," Nucl. Eng. Dept. Report UWFDM-112 (Univ. of Wisconsin, Nov. 1975), Chapter II.

16. R. W. Conn, J. Kesner, Nuclear Fusion 15, 775 (1975).

17. M. Ohta, H. Yamato, S. Mori, "Thermal Instability and Control of Fusion Reactor," in Plasma Physics and Controlled Nuclear Fusion Research (Proc. 4th Int. Conf Madison, 1971) 3, IAEA Vienna (1971) 423.

18. A. T. Mense, G. A. Emmert, J. D. Callen, Nucl. Fusion 15, (1975) 703.

19. S. L. Gralnick, Nucl. Fusion 13 (1973) 703.

20. W. M. Stacey, Jr., Nuclear Fusion 15 (1975) 63.

Table 1A †

	a (m)	$\bar{T}_i$ (keV)	T_{max} (keV)	T_{min} (keV)	$\bar{n}$ (cm^{-3})	n_{min} (cm^{-3})	n_{max} (cm^{-3})
a	5	8.5	14.6	2.9	4×10^{13}	3.7×10^{12}	1.7×10^{14}
b	5	10.9	20.3	3.7	5×10^{13}	4.7×10^{12}	2.2×10^{14}
c	5	13.1	26.0	4.2	6×10^{13}	5.5×10^{12}	2.75×10^{14}
d	4	8.8	15.1	3.5	7×10^{13}	1.03×10^{13}	2.5×10^{14}
e	4	10.5	19.0	4.0	8×10^{13}	1.2×10^{13}	3.0×10^{14}

Table 1B †

	a (m)	P_α (MW)	r_p/a *	τ_E (sec)	τ_p (sec)	Fractional Burnup	Fueling Rate (sec^{-1})
a	5	390	.40	3.7	1.25	.60%	2.3×10^{23}
b	5	1090	.40	2.4	.69	.74%	5.2×10^{23}
c	5	2190	.40	1.7	.48	.84%	9.3×10^{23}
d	4	576	.43	2.4	.91	.71%	2.9×10^{23}
e	4	1130	.45	1.8	.59	.81%	5.0×10^{23}

* r_p = radius within which 90% of fusion power is generated

† Aspect ratio is 3, q(a) is 2.5, and B_T = 40 kG in all cases.

Table 2

	$\bar{T}_i$ (keV)	T_{min} (keV)	T_{max} (keV)	n_{max} (cm^{-3})	n_{min} (cm^{-3})	P_α (MW)	τ_E (sec)	τ_p (sec)
1	11.1	2.3	20.9	2.1×10^{14}	5×10^{12}	1080	2.4	.73
2	13.4	3.3	29.9	1.2×10^{14}	2×10^{13}	877	3.5	2.0
3	25.4	6.9	58.3	7.15×10^{13}	4×10^{13}	1390	3.9	8.0

In all these calculations, a = 5 m, $\bar{n} = 5 \times 10^{13}$, A = 3, B_T = 40 kG, q(a) = 2.5, $L_e = L_i$ = 50 cm.

Table 3

	Space-Time	Global Balance
Tokamak minor radius (m)	5	5
Aspect Ratio	3	3
Toroidal field on axis (kG)	40	40
Safety factor at plasma edge, q(a)	2.5	2.5
Mean ion density (cm^{-3})	4×10^{13}	4.0×10^{13}
Mean electron density (cm^{-3})	4.1×10^{13}	4.2×10^{13}
Mean alpha density (cm^{-3})	3.5×10^{11}	1.1×10^{12}
Mean electron temperature	8.8	20.2
Mean ion temperature	8.45	16.5
Electron poloidal beta, β_{θ_e}	.51	1.15
Total poloidal beta, β_θ	1.15	2.46
Total toroidal beta, β_ϕ	.021	.044
Energy content of plasma (GJ)	1.4	3.1
Particle containment time (sec)	1.25	5.8
Energy containment time (sec)	3.7	2.9
$\bar{n}_e \tau_E$	1.5×10^{14}	1.2×10^{14}
Fractional burnup	.60%	5.4%
Total thermal power (17.6 MeV/fusion),(GW)	1.97	4.2
Average power density in plasma (W/cm^3)	.053	.037
Tritium (deuterium) consumption rate (sec^{-1})	7.0×10^{20}	1.5×10^{21}
Particle leakage rate (D+T+α) (sec^{-1})	2.3×10^{23}	5.24×10^{22}

Figure Captions

Fig. 1 - Lawson criteria for the energy containment time necessary to "break-even" for a driven reactor, calculated for various density and temperature profiles. The peakedness of these profiles is characterized by the factor δ.

Fig. 2 - The ignition-criteria for the energy containment time necessary to "ignite" a plasma, calculated for various density and temperature profiles.

Fig. 3 - The mean fusion power density as a function of mean temperature for a tokamak-like plasma where a beta limit is imposed. The density and temperature profiles are allowed to vary and their shape is characterized by the parameter δ.

Fig. 4 - Temperature and density profiles attained in a 5 m minor radius tokamak. Below a mean density of $4 \times 10^{13}\ cm^{-3}$ no thermally stable ignited equilibria are found.

Fig. 5 - Ion, electron and alpha density profiles for an ignited, thermally stable, 5 m minor radius tokamak.

Fig. 6 - Profile of diffusion coefficient for three cases of a stable 5 m minor radius tokamak.

Fig. 7 - The total poloidal beta vs. mean ion temperature for a 4 and 5 m minor radius tokamak. The dashed portion of the curve represents the region in which MHD equilibrium would not be expected to exist. Below the ignition cutoff, no ignited solutions are found.

Fig. 8 - (a) Equilibrium density profiles for a mean density of 5×10^{13} and an edge density of 5×10^{12}, 2×10^{13} and 4×10^{13} respectively. (b) Convective loss rate for deutrons and tritons at the plasma edge as a function of the plasma edge density.

Fig. 9 - Mean poloidal beta as a function of the edge to axis source density. The source shape varies from being parabolic to being spacially independent.

Fig. 10 - Variation of the mean poloidal beta for sources that are peaked near to the plasma edge.

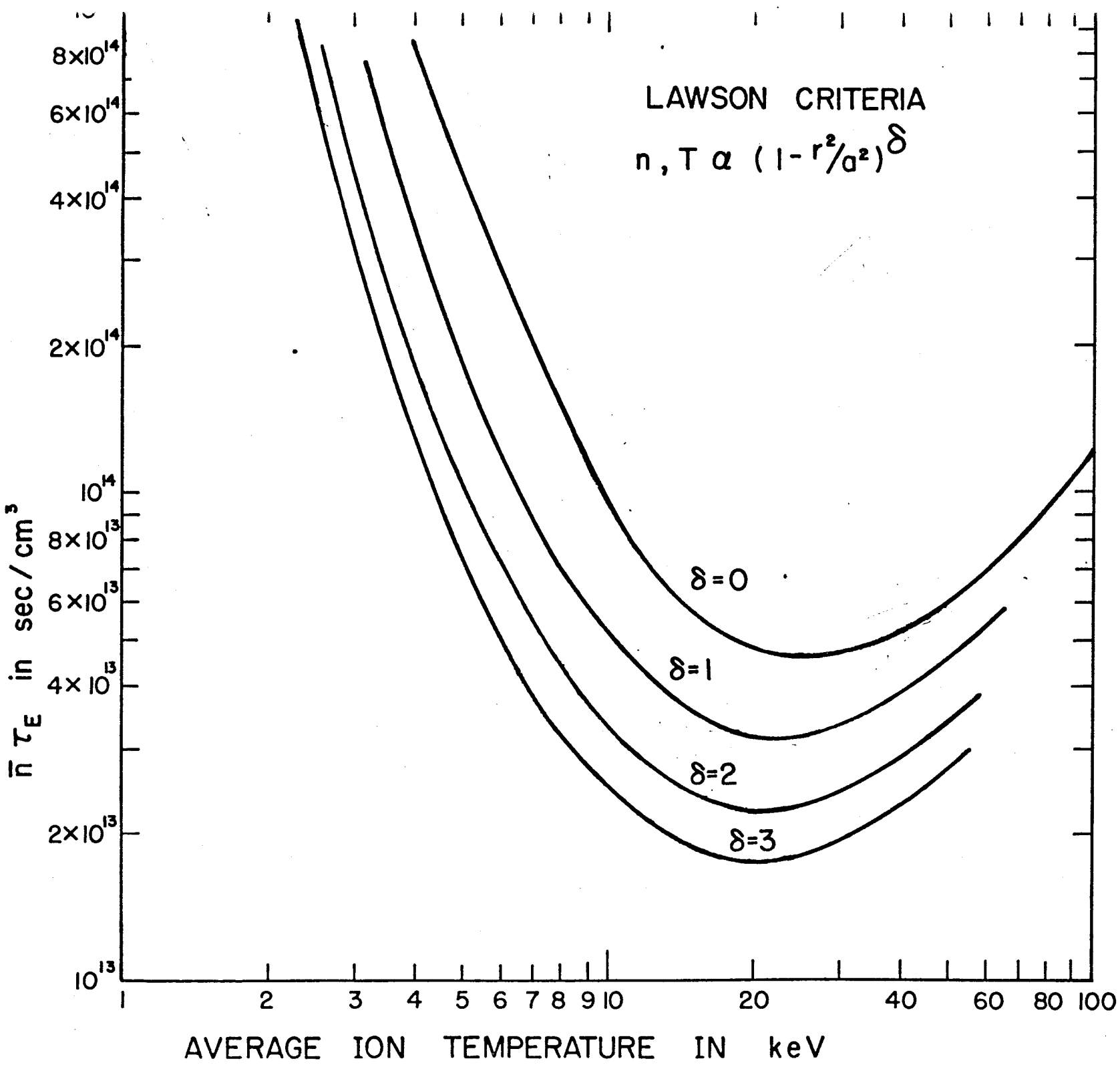
LAWSON CRITERIA
n, T α (1 - r²/a²)^δ
δ=0
δ=1
δ=2
δ=3
8×10^14
6×10^14
4×10^14
2×10^14
10^14
8×10^13
6×10^13
4×10^13
2×10^13
10^13
n̄ τ_E in sec/cm³
1
2
3
4
5
6
7
8
9
10
20
40
60
80
100
AVERAGE ION TEMPERATURE IN keV

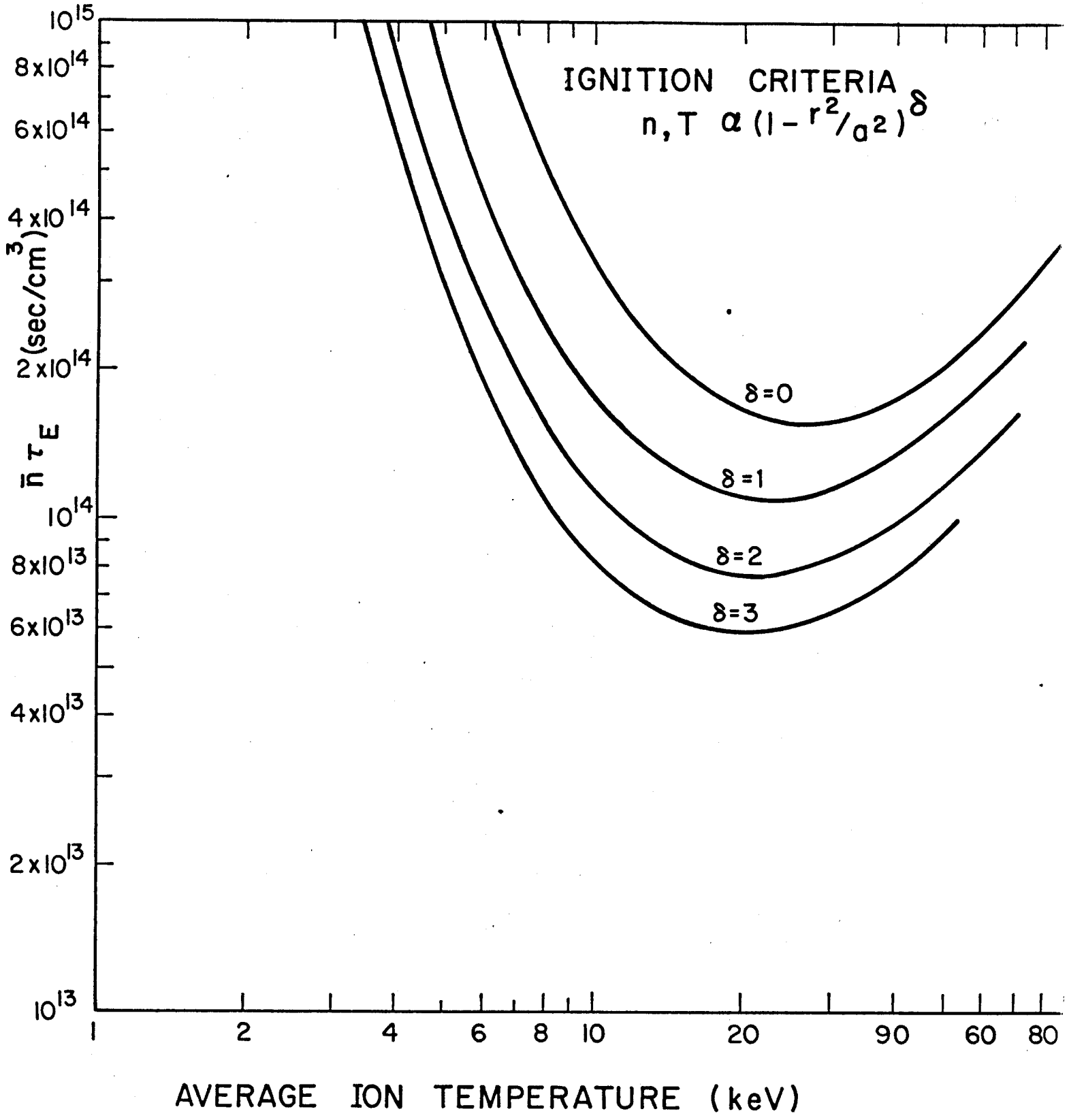
IGNITION CRITERIA
n, T α (1 − r²/a²)^δ
δ=0
δ=1
δ=2
δ=3
$\bar{n}\tau_E$ (sec/cm³)
10¹⁵
8x10¹⁴
6x10¹⁴
4x10¹⁴
2x10¹⁴
10¹⁴
8x10¹³
6x10¹³
4x10¹³
2x10¹³
10¹³
1
2
4
6
8
10
20
90
60
80
AVERAGE ION TEMPERATURE (keV)

FIGURE 2

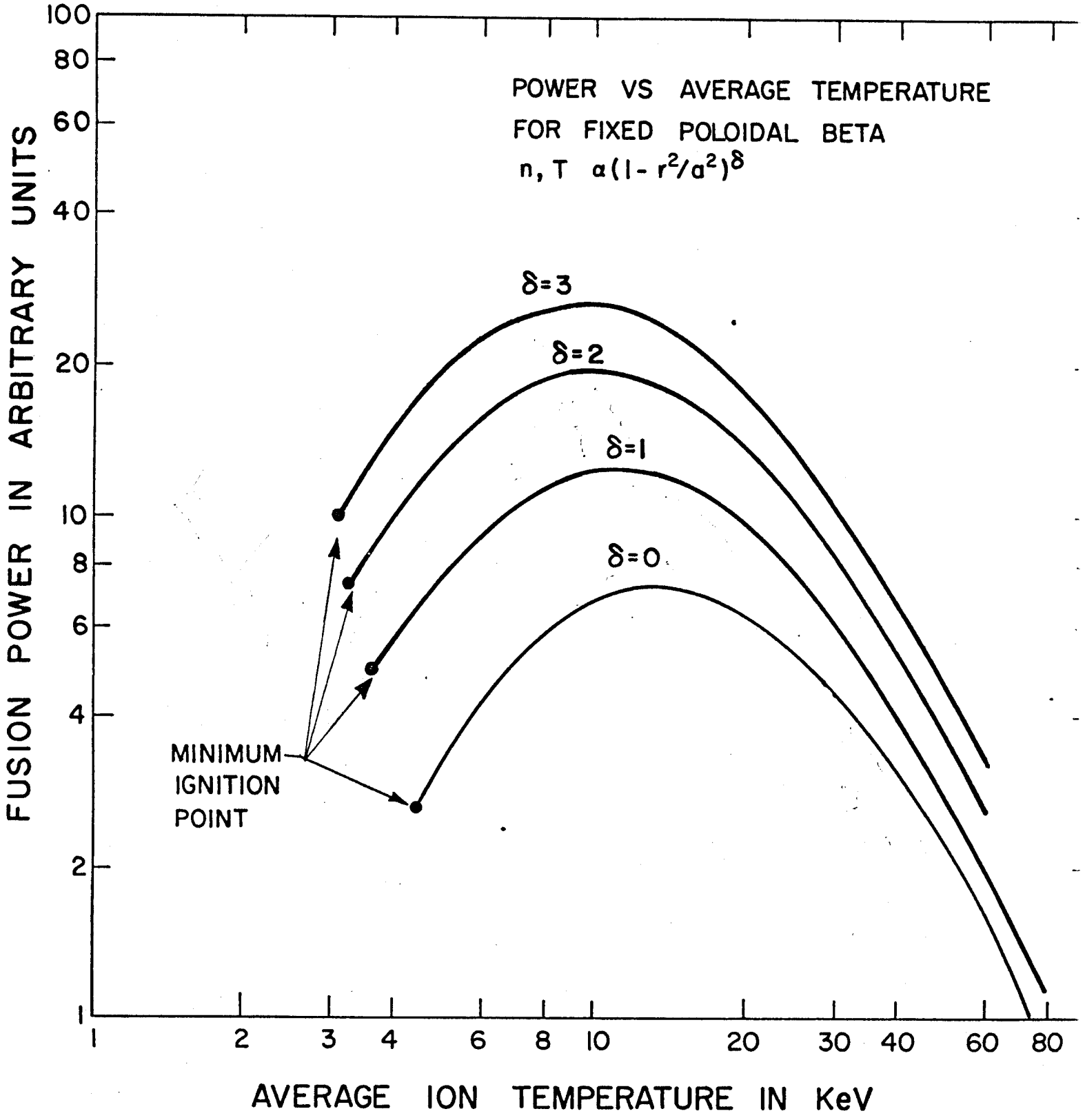
POWER VS AVERAGE TEMPERATURE
FOR FIXED POLOIDAL BETA
n, T α(1 - r²/a²)^δ
δ=3
δ=2
δ=1
δ=0
MINIMUM
IGNITION
POINT
FUSION POWER IN ARBITRARY UNITS
100
80
60
40
20
10
8
6
4
2
1
1
2
3
4
6
8
10
20
30
40
60
80
AVERAGE ION TEMPERATURE IN KeV

FIGURE 3

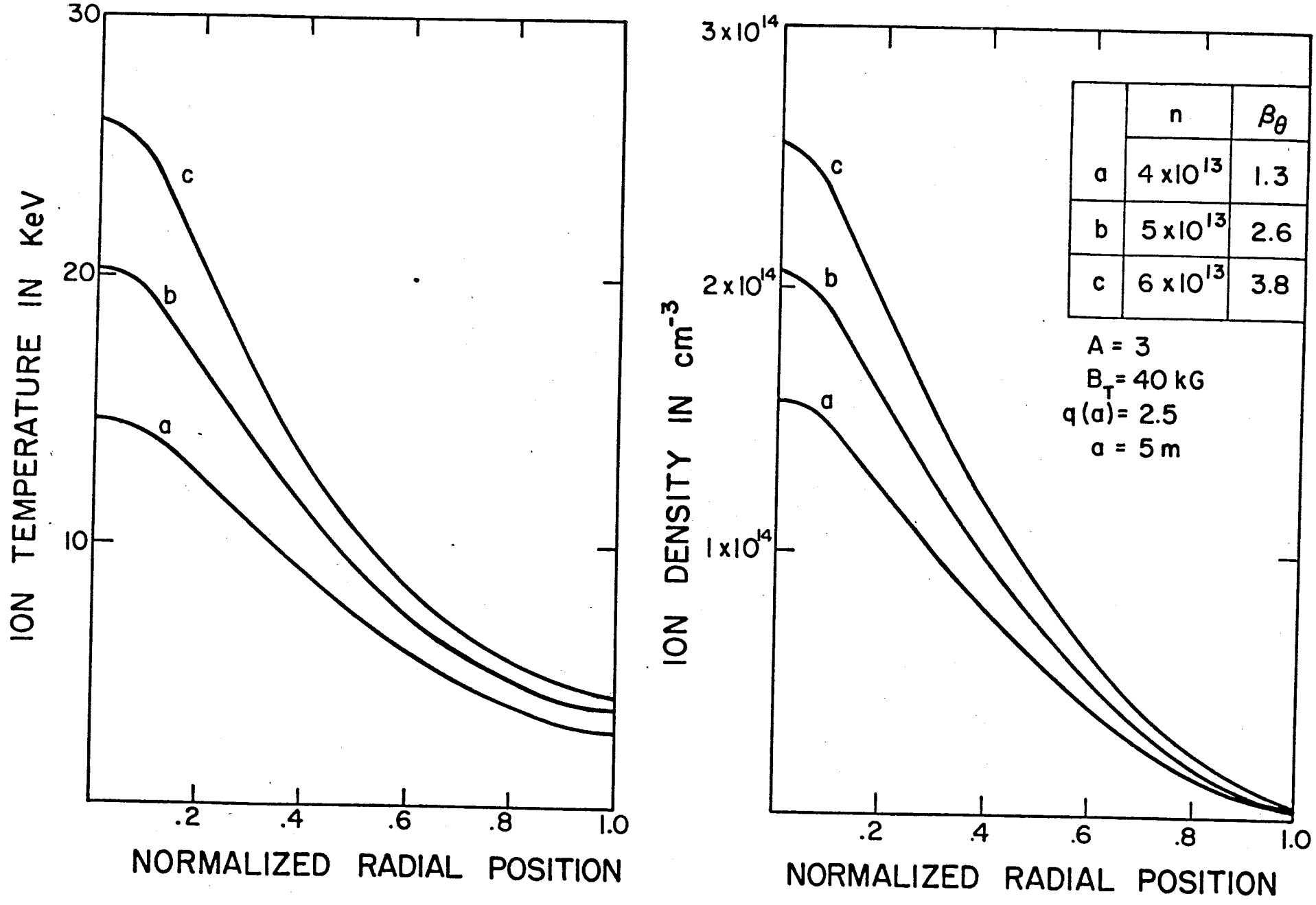
30
20
10
ION TEMPERATURE IN KeV
c
b
a
.2
.4
.6
.8
1.0
NORMALIZED RADIAL POSITION
3x10^14
2x10^14
1x10^14
ION DENSITY IN cm^-3
n
β_θ
a
4 x10^13
1.3
b
5 x10^13
2.6
c
6 x10^13
3.8
A = 3
B_T = 40 kG
q(a) = 2.5
a = 5 m
NORMALIZED RADIAL POSITION

FIGURE 4

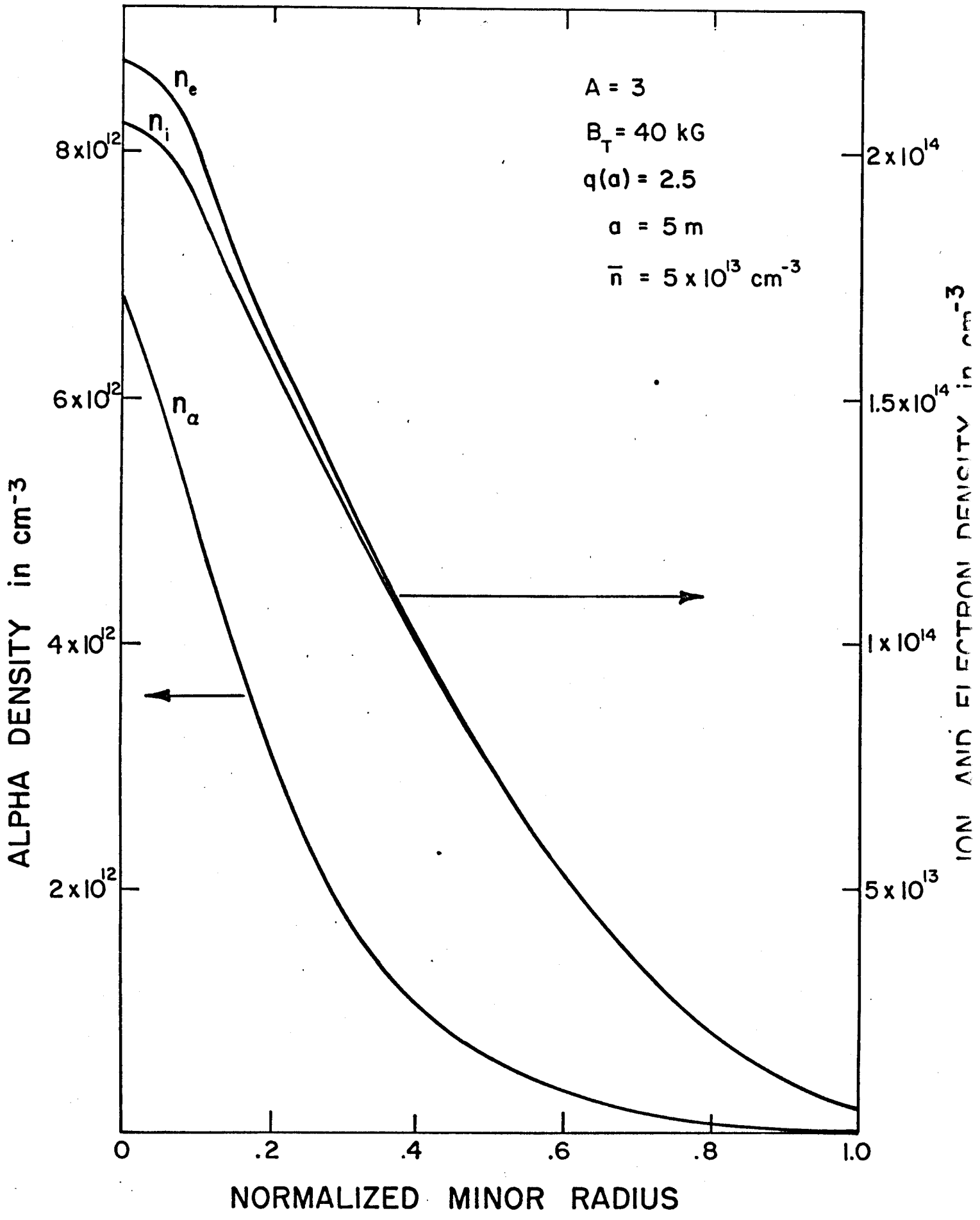
A = 3
B_T = 40 kG
q(a) = 2.5
a = 5 m
$\bar{n}$ = 5 x 10^{13} cm^{-3}
n_e
n_i
n_α
8×10^{12}
6×10^{12}
4×10^{12}
2×10^{12}
2×10^{14}
1.5×10^{14}
1×10^{14}
5×10^{13}
ALPHA DENSITY in cm^{-3}
ION AND ELECTRON DENSITY in cm^{-3}
0
.2
.4
.6
.8
1.0
NORMALIZED MINOR RADIUS

FIGURE 5

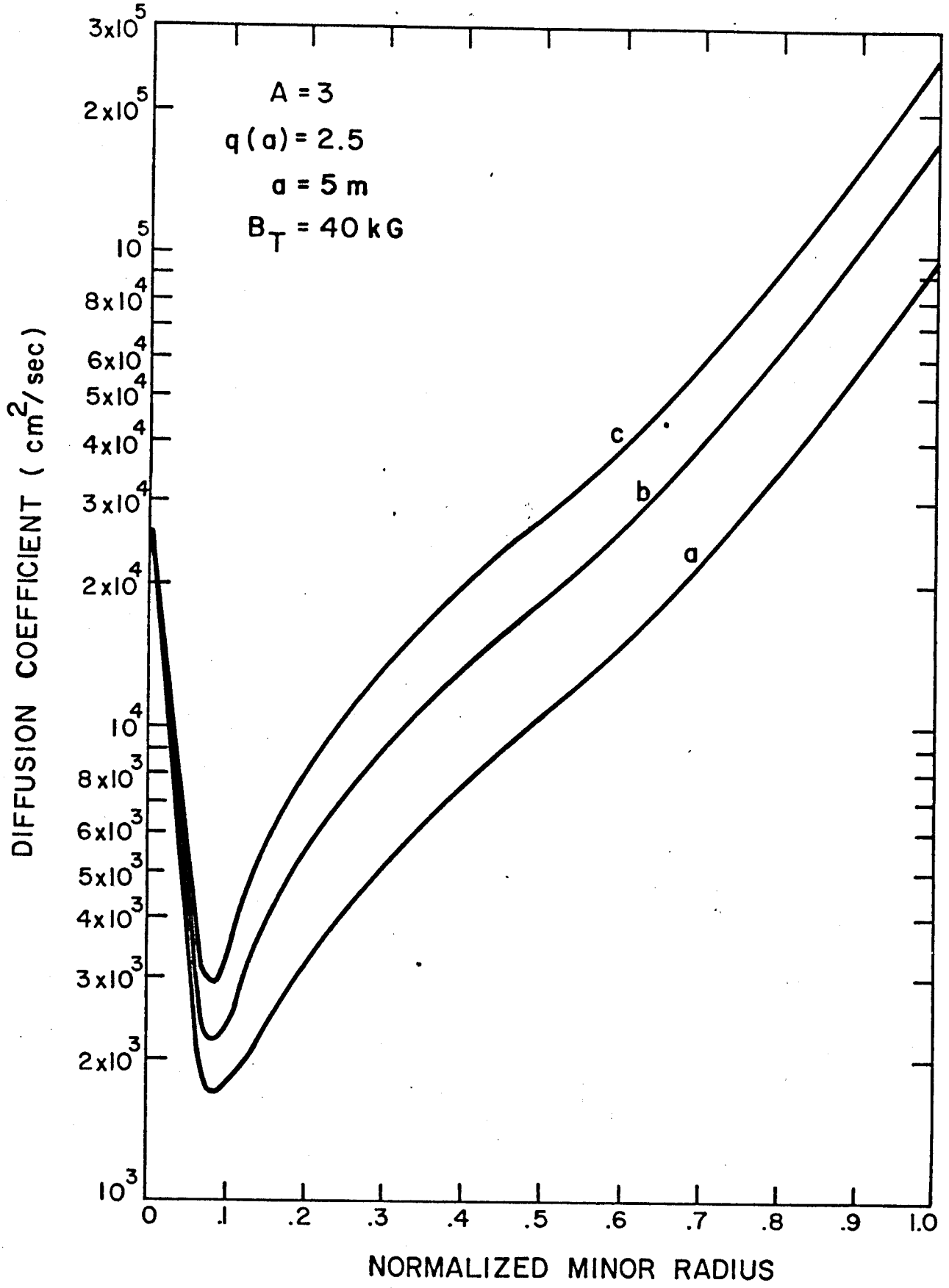
A = 3
q(a) = 2.5
a = 5 m
B_T = 40 kG
c
b
a
DIFFUSION COEFFICIENT (cm^2/sec)
NORMALIZED MINOR RADIUS
$3x10^5$
$2x10^5$
10^5
$8x10^4$
$6x10^4$
$5x10^4$
$4x10^4$
$3x10^4$
$2x10^4$
10^4
$8x10^3$
$6x10^3$
$5x10^3$
$4x10^3$
$3x10^3$
$2x10^3$
10^3
0
.1
.2
.3
.4
.5
.6
.7
.8
.9
1.0

FIGURE 6

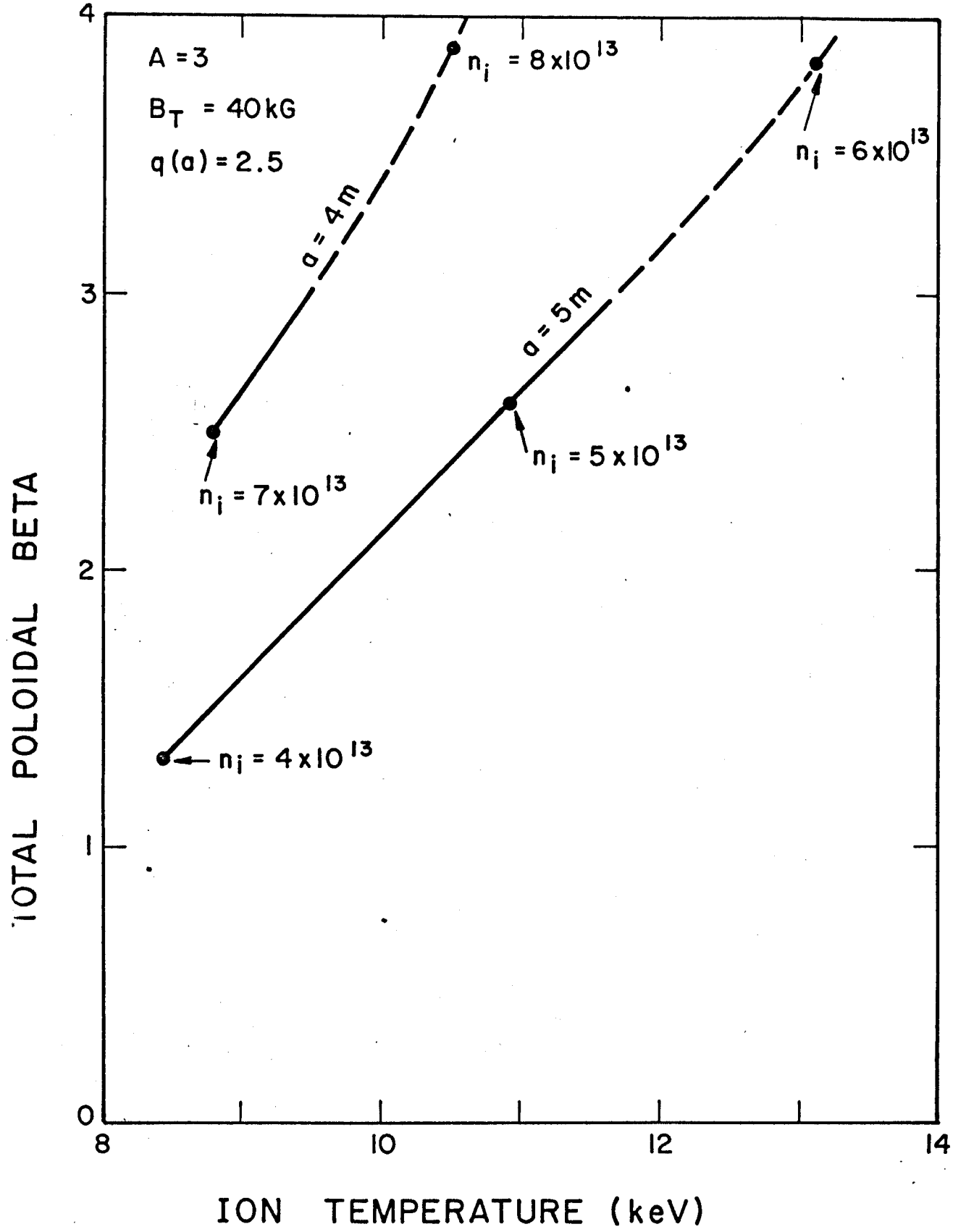
A = 3
B_T = 40kG
q(a) = 2.5
a = 4m
a = 5m
$n_i = 8 \times 10^{13}$
$n_i = 6 \times 10^{13}$
$n_i = 7 \times 10^{13}$
$n_i = 5 \times 10^{13}$
$n_i = 4 \times 10^{13}$
TOTAL POLOIDAL BETA
ION TEMPERATURE (keV)
0
1
2
3
4
8
10
12
14

FIGURE 7

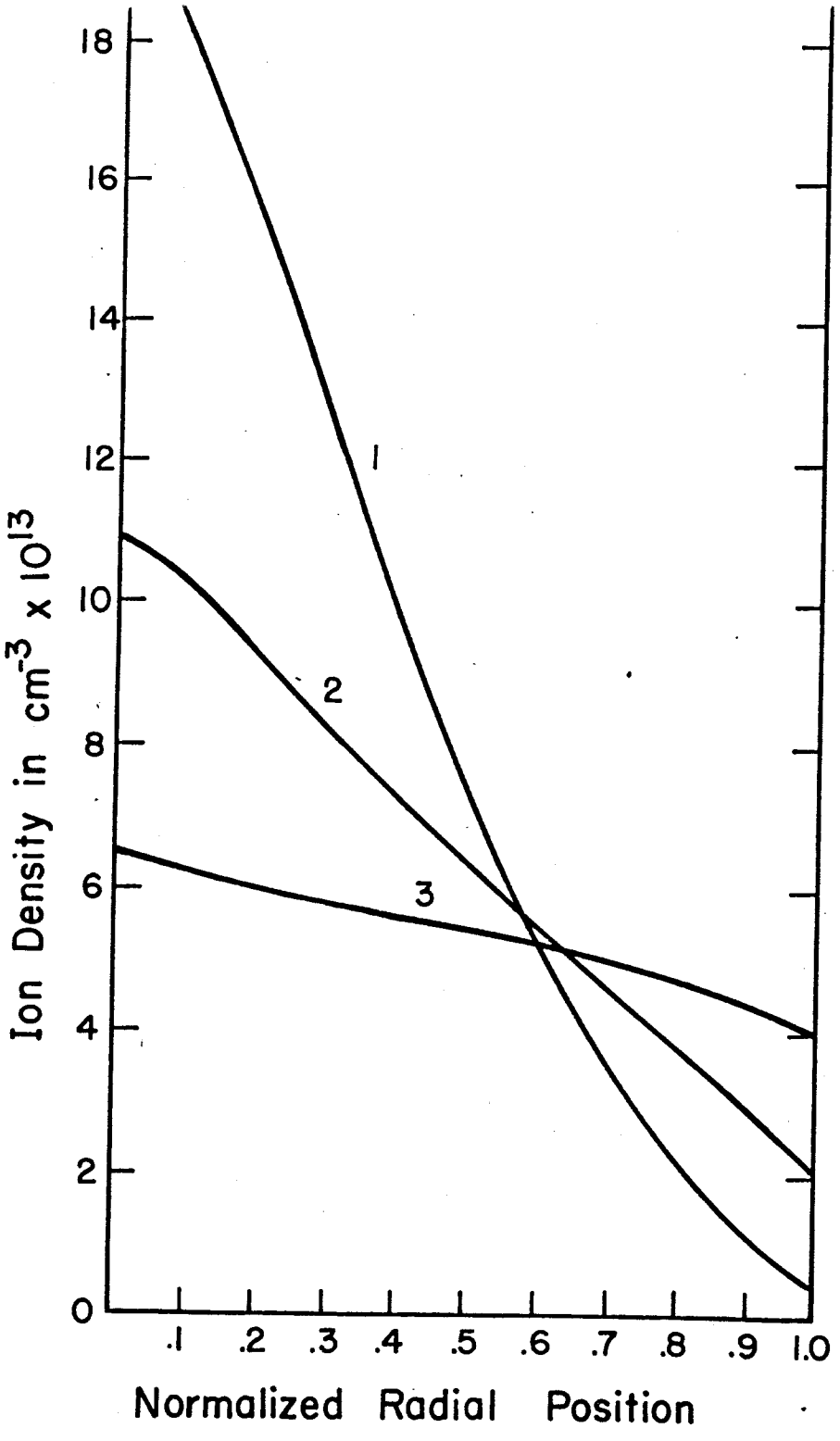
Ion Density in cm^{-3} x 10^{13}
Normalized Radial Position
0
2
4
6
8
10
12
14
16
18
.1
.2
.3
.4
.5
.6
.7
.8
.9
1.0
1
2
3

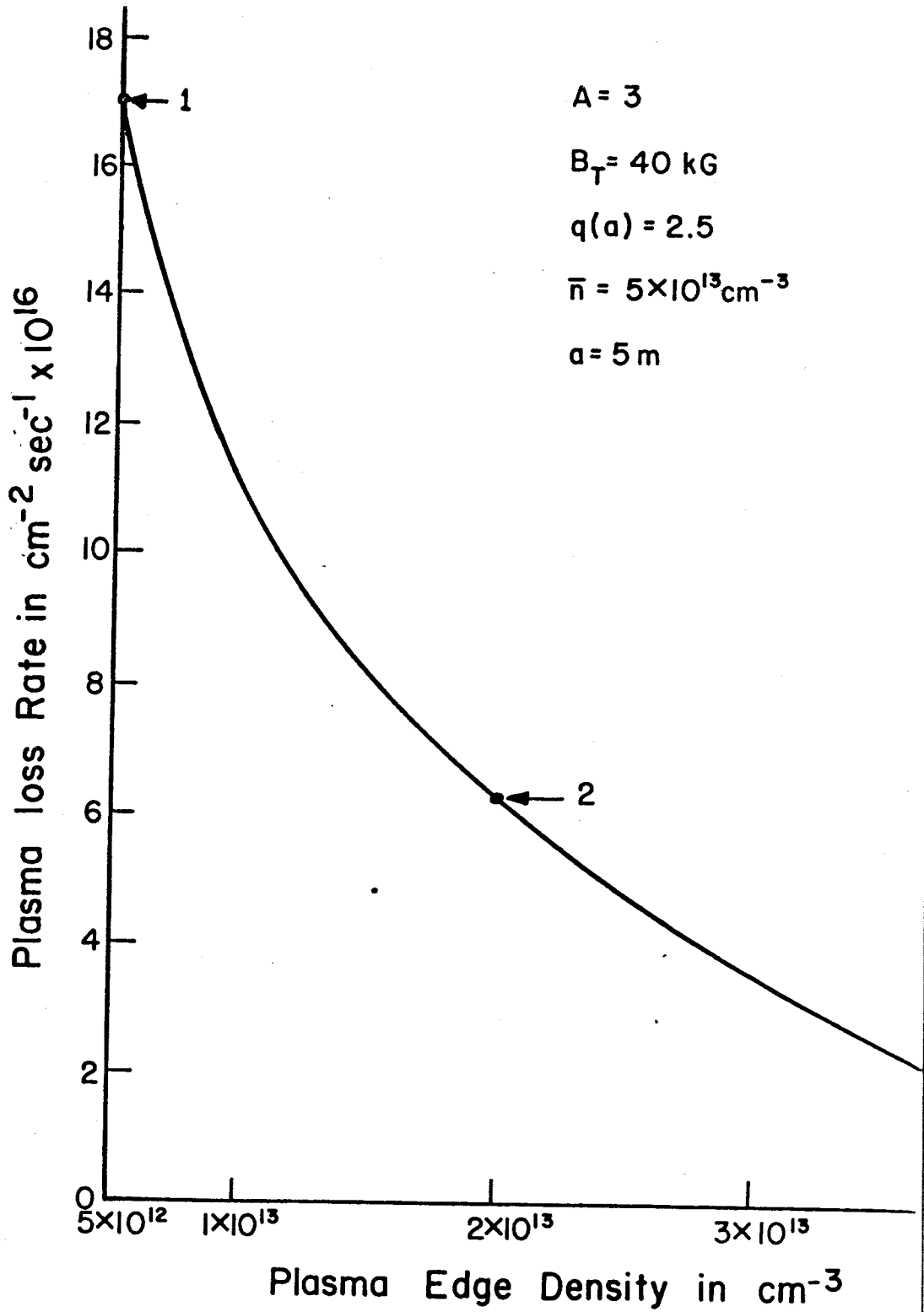
Plasma loss Rate in cm^{-2} sec^{-1} x 10^{16}
Plasma Edge Density in cm^{-3}
A = 3
B_T = 40 kG
q(a) = 2.5
$\bar{n}$ = $5\times10^{13}cm^{-3}$
a = 5 m
0
2
4
6
8
10
12
14
16
18
5×10^{12}
1×10^{13}
2×10^{13}
3×10^{13}
1
2

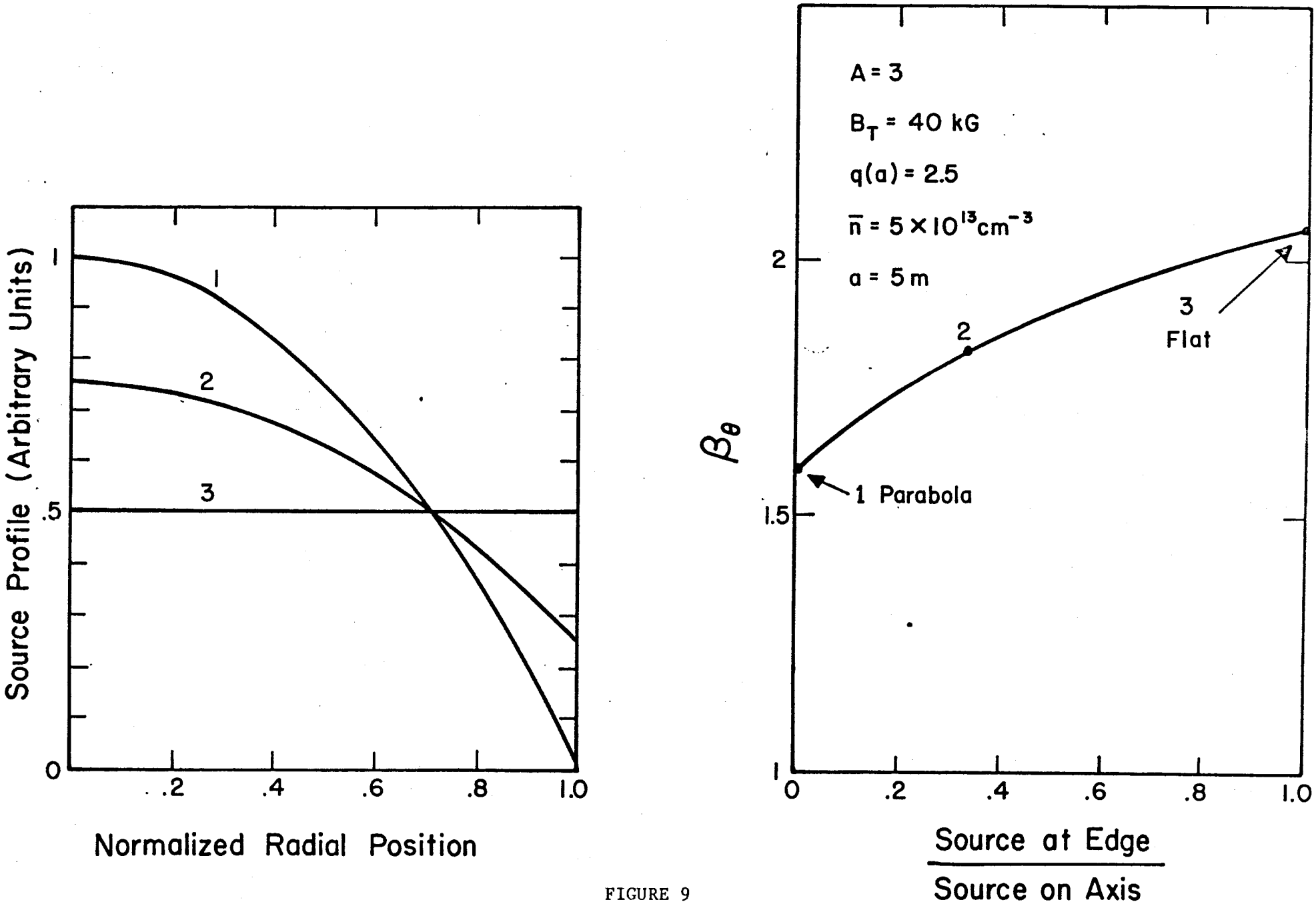
A = 3
B_T = 40 kG
q(a) = 2.5
$\bar{n} = 5 \times 10^{13} cm^{-3}$
a = 5 m
β_θ
1 Parabola
2
3
Flat
Source at Edge
Source on Axis
Source Profile (Arbitrary Units)
Normalized Radial Position
1
2
3
0
.5
1
1.5
2
.2
.4
.6
.8
1.0

FIGURE 9

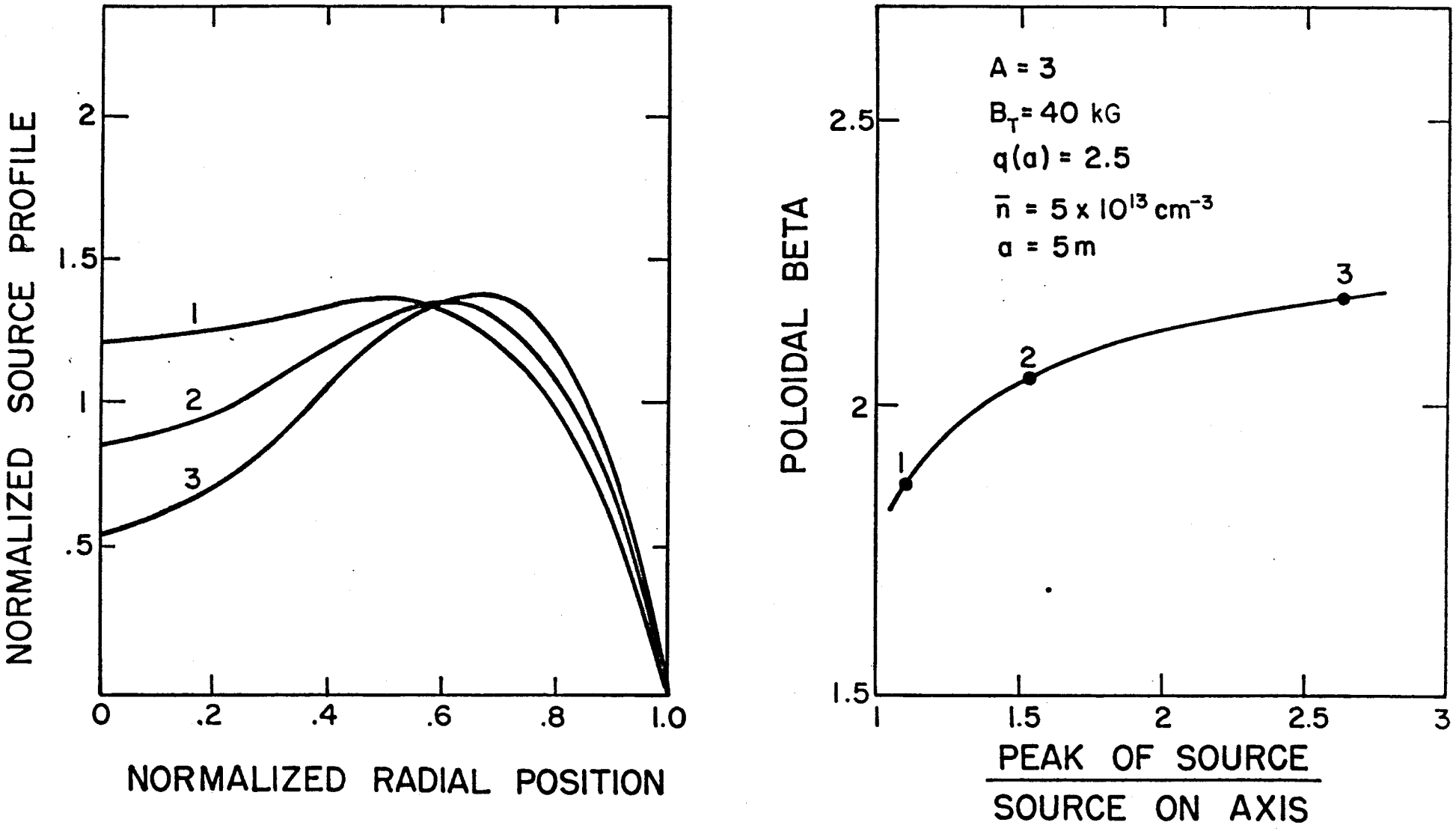
NORMALIZED SOURCE PROFILE
2
1.5
1
.5
0
.2
.4
.6
.8
1.0
1
2
3
NORMALIZED RADIAL POSITION
A = 3
B_T = 40 kG
q(a) = 2.5
$\bar{n}$ = 5 x 10^{13} cm^{-3}
a = 5m
POLOIDAL BETA
2.5
2
1.5
1
1.5
2
2.5
3
1
2
3
PEAK OF SOURCE
SOURCE ON AXIS

FIGURE 10